Articles

MultiFunctional Molecular Scratchcards

L. G. Harris, W. C. E. Schofield, and J. P. S. Badyal*

Department of Chemistry, Science Laboratories, Durham University, Durham DH1 3LE, United Kingdom

Received October 16, 2006. Revised Manuscript Received January 24, 2007

Plasmachemical nanolayering in combination with localized removal of an upper passivation layer is shown to be a simple route for the fabrication of patterned functional surfaces. Protein and DNA arrays can be prepared utilizing a dual layer structure in which the outer layer is nonbinding, and the exposed underlayer specifically immobilizes the respective biomolecule.

1. Introduction

Functional patterning of solid surfaces is of key importance for technological applications such as thin film transistors,[1] solar cells,[2] genomics,[3−5] proteomics,[6−8] microelectronics,[9−11] sensors,[12] and microfluidics.[13−15] A plethora of techniques has been devised for this purpose on the basis of top down, bottom up, or a combination of both approaches.[16,17] These include light stamping,[18] microcontact printing,[19−23] microarraying,[24−26] e-beam lithography,[27−29] polymer blend phase separation,[30−32] laser writing,[33−35] and exposure through a mask to a reactive medium.[36−38] Most recently, the utilization of scanning probe tips for patterning on the nanoscale has emerged as a promising alternative. This encompasses dip pen nanolithography,[39−41] electro pen nanolithography,[42] local anodic oxidation,[43−47] nanoshaving,[48−53] and thermal scrib-

* To whom correspondence should be addressed. E-mail: j.p.badyal@durham.ac.uk.

(1) Whang, Z.; Zhang, J.; Xing, R.; Yuan, J.; Yan, D.; Han, Y. *J. Am. Chem. Soc.* **2003**, *125*, 15278.
(2) Jiang, P.; McFarland, M. J. *J. Am. Chem. Soc.* **2005**, *127*, 3710.
(3) Peterlinz, K. A.; Georgiadis, R. M.; Herne, Tarlov M. J. *J. Am. Chem. Soc.* **1997**, *119*, 3401.
(4) Schena, M.; Shalon, D.; Davis, R. W.; Brown, P. O. *Science* **1995**, *270*, 467.
(5) Georgiadis, R.; Peterlinz, K. P.; Peterson, A. W. *J. Am. Chem. Soc.* **2000**, *122*, 3166.
(6) MacBeath, G.; Schreiber, S. L. *Science* **2000**, *289*, 1760.
(7) Kane, R. S.; Takayama, S.; Ostuni, E.; Ingber, D. E.; Whitesides, G. M. *Biomaterials* **1999**, *20*, 2363.
(8) Zhou, H.; Baldini, L.; Hong, J.; Wilson, A. J.; Hamilton, A. D. *J. Am. Chem. Soc.* **2006**, *128*, 2421.
(9) Zhong, Z.; Wang, D.; Cui, Y.; Bockrath, M. W.; Lieber, C. M. *Science* **2003**, *302*, 1377.
(10) Filho, F. H. D.; Mauricio, M. H. P.; Ponciano, C. R.; Prioli, R. *Mater. Sci. Eng., B* **2004**, *112*, 194.
(11) Wallraff, G. M.; Hinsberg, W. D. *Chem. Rev.* **1999**, *99*, 1801.
(12) Wei, C.; Dai, L.; Roy, A.; Tolle, T. B. *J. Am. Chem. Soc.* **2006**, *128*, 1412.
(13) Kline, R. T.; Paxton, F. W.; Wang, Y.; Velegol, D.; Mallouk, T. E.; Sen, A. *J. Am. Chem. Soc.* **2005**, *127*, 17150.
(14) Beebe, D. J.; Moore, J. S.; Yu, Q.; Liu, R.; Kraft, M. L.; Jo, B.; Devadoss, C. *Proc. Natl. Acad. Sci.* **2000**, *97*, 13488.
(15) Beebe, D. J.; Mensing, G. A.; Walker, G. M. *Ann. Rev. Biomed. Eng.* **2002**, *4*, 261.
(16) Heath, J. R. *Acc. Chem. Res.* **1999**, *32*, 388.
(17) Du, P.; Mingqi, L.; Douki, K.; Li, X.; Garcia, C. B. W.; Jain, A.; Smilgies D. M.; Fetters L. J.; Gruner, S. M.; Wiesner, U.; Ober, C. K. *Adv. Mater.* **2004**, *16*, 953.
(18) Park, K. S.; Seo, E. K.; Do, Y. R.; Kim, K.; Sung, M. M. *J. Am. Chem. Soc.* **2006**, *128*, 858.
(19) Xia, Y.; Whitesides, G. M. *Angew. Chem., Int. Ed.* **1998**, *37*, 550.
(20) Lackowski, W. M.; Ghosh, P.; Crooks, R. M. *J. Am. Chem. Soc.* **1999**, *121*, 1419.
(21) Tan, J. L.; Tien, J.; Chen, C. S. *Langmuir* **2002**, *18*, 519.
(22) Yu, A. A.; Savas, T.; Cabrini, S.; diFabrizio, E.; Smith, H. I.; Stellacci, F. *J. Am. Chem. Soc.* **2005**, *127*, 16774.
(23) Langowski, B. A.; Uhrich, K. E. *Langmuir* **2005**, *21*, 10509.
(24) Rupcich, N.; Goldstein, A.; Brennan, J. D. *Chem. Mater.* **2003**, *15*, 1803.
(25) Lin, H.; Sun, L.; Crooks, R. M. *J. Am. Chem. Soc.* **2005**, *127*, 11210.
(26) MacBeath, G.; Koehler, A. N.; Schreiber, S. L. *J. Am. Chem. Soc.* **1999**, *121*, 7967.
(27) Mendes, P. M.; Jacke, S.; Critchley, K.; Plaza, J.; Chen, Y.; Nikitin, K.; Palmer, R. E.; Preece, J. A.; Evans, S. D.; Fitzmaurice, D. *Langmuir* **2004**, *20*, 3766.
(28) Sondag-Huethorst, J. A. M.; Fokkink, L. G. *Langmuir* **1995**, *11*, 4823.
(29) Kim, J. M.; Jung, H. S.; Park, J. W.; Yukimasa, T.; Oka, H.; Lee, H. Y.; Kawai, T. *J. Am. Chem. Soc.* **2005**, *127*, 2358.
(30) Zhao, B.; Zhu, L. *J. Am. Chem. Soc.* **2006**, *128*, 4574.
(31) Wang, C. W.; Moffit, M. G. *Chem. Mater.* **2005**, *17*, 3871.
(32) Minelli, C.; Hinderling, C.; Heinzelmann, H.; Pugin, R.; Liley, M. *Langmuir* **2005**, *21*, 7080.
(33) Behm, J. M.; Lykke, K. R.; Pellin, M. J.; Hemminger, J. C. *Langmuir* **1996**, *12*, 2124.
(34) Anderson, J. R.; Chiu, D. T.; Jackmann, R. J.; Cherniavskaya, O.; McDonald, J. C.; Wu, H.; Whitesides, S. H.; Whitesides, G. M. *Anal. Chem.* **2000**, *72*, 3158.
(35) Zhou, C.; Nagy, G.; Walker, A. V. *J. Am. Chem. Soc.* **2005**, *127*, 12160.
(36) Lejeune, M.; Valsesia, A.; Kormunda, M.; Colpo, P.; Rossi, F. *Surf. Sci.* **2005**, *583*, L142.
(37) Choi, Y. K.; Zhu, J.; Grunes, J.; Bokor, J.; Somorjai, G. A. *J. Phys. Chem. B* **2003**, *107*, 3340.
(38) Korczagin, I.; Golze, S.; Hempenius M. A.; Vansco, G. J. *Chem. Mater.* **2003**, *15*, 3663.
(39) Davis, J. J.; Coleman, K. S.; Busuttil, K. L.; Bagshaw, C. B. *J. Am. Chem. Soc.* **2005**, *127*, 13082.
(40) Ginger, D. S.; Zhang, H.; Mirkin, C. A. *Angew. Chem., Int. Ed.* **2004**, *43*, 30.
(41) Lee, K. B.; Lin, J. H.; Mirkin, C. A. *J. Am. Chem. Soc.* **2003**, *125*, 5588.
(42) Cai, Y.; Ocko, B. M. *J. Am. Chem. Soc.* **2005**, *127*, 16287.
(43) Xie, X. N.; Deng, M.; Xu, H.; Yang, S. W.; Qi, D. C.; Gao, X. Y.; Chung, H. J.; Sow, C. H.; Tan, V. B. C.; Wee, T. S. W. *J. Am. Chem. Soc.* **2006**, *128*, 2738.
(44) Tella, M.; Garcia, R. *Appl. Phys. Lett.* **2001**, *79*, 424.
(45) Dagata, J. A.; Scheir, J.; Harary, H. H.; Evans, C. J.; Postek, M. T.; Bennet, J. *Appl. Phys. Lett.* **1990**, *56*, 2001.

10.1021/cm0624670 CCC: $37.00
Published on Web 03/13/2007

Scheme 1. Molecular Scratchcard Fabrication Followed by Either Robotic Micropin Puncturing or SPM Tip Scratching

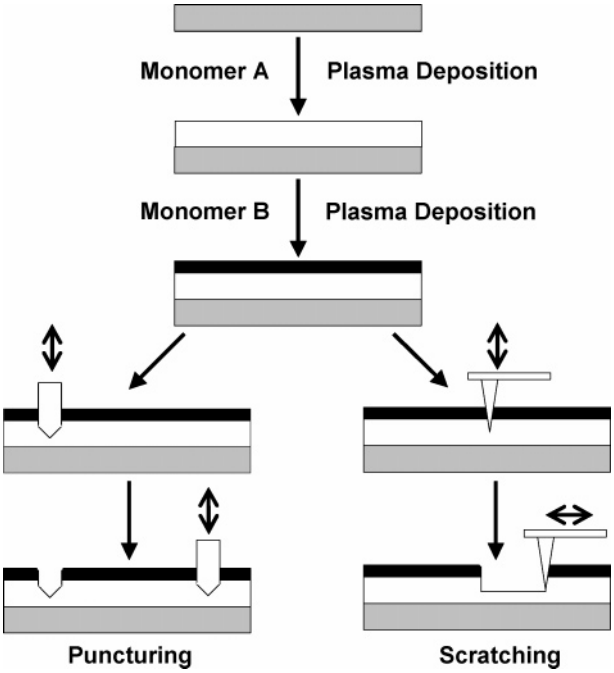

ing.[54,55] Generically, such scanning probe patterning techniques comprise either direct surface modification or partial removal of a surface layer to reveal the underlying substrate (which can then be subjected to further functionalization). Dip pen nanolithography[39−41] is an example of the former approach, in which ink is transferred from a scanning probe tip onto a surface; associated drawbacks include the prerequisite of tip modification prior to use and the reliance on specific ink−substrate interactions (e.g., gold−thiol coupling for the generation of self-assembled monolayers (SAMs)[56−60]). The alternative variant, in which SAMs are directly removed by the tip,[48−53] also suffers from substrate specificity and poor shelf life attributable to the low Au−S bond enthalpy triggering oxidation and desorption processes at the gold surface.[61]

In this article, we outline a new and relatively straightforward approach for chemically patterning solid surfaces on both the micro- and nanoscales, which is based on plasmachemical nanolayering to construct multifunctional stacks and subsequent nanoscale scratching or puncturing down to the appropriate depth in order to expose the desired functionality, Scheme 1.

Previous attempts to fabricate multilayer functional stacks have tended to be cumbersome and reliant upon complex and expensive syntheses.[62] The major attributes envisaged in the present case include the absence of multistep solvent-based surface functionalization chemistries, substrate independence (i.e., applicable to metal, inorganic, or polymer substrates), high throughput capabilities, and the scope for fabricating multifunctional (multiplex) surfaces. The utilization of plasma deposition ensures covalent bonding of the multilayer stack to the substrate via free radical sites created at the interface during the onset of electrical discharge exposure. Appropriate choice of functional gaseous precursors (containing polymerizable carbon−carbon double bonds) in combination with electric discharge modulation on millisecond−microsecond time scales makes it possible to easily build up multifunctional stacks. The well-defined nanolayers stem from the short pulsed plasma duty cycle on-time (microseconds) generating active sites in the gas phase and also at the growing film surface via UV irradiation or ion or electron bombardment, followed by conventional polymerization processes operating throughout the prolonged off-time (milliseconds) in the absence of any UV-, ion-, or electron-induced damage.[63,64] Extremely high levels of surface functionality for each pulsed plasma nanolayer can be achieved using this approach, as a consequence of precursor structural retention. Furthermore, by programming the pulse duty cycle, we can tailor the surface density of desired chemical groups (which is a distinct advantage compared to conventional surface functionalization techniques). Examples successfully devised in the past include amine,[65] anhydride,[64] epoxide,[66] carboxylic acid,[67] cyano,[68] halide,[69] hydroxyl,[70] furfuryl,[71] perfluoroalkyl,[72] and thiol[73] groups. In the present investigation, functional nanolayering

(46) Dagata, J. A.; Perez-Murano, F.; Abadal, G.; Morimoto, K.; Inoue, T.; Itoh, J.; Yokoyama, H. *Appl. Phys. Lett.* **2000**, *76*, 2710.
(47) Martin, C.; Rius, G.; Borrrise, X.; Perez-Murano, F. *Nanotechnology* **2005**, *16*, 1016.
(48) Seo, K.; Borguet, E. *Langmuir* **2006**, *22*, 1388.
(49) Sung, I. H.; Kim, D. E.; *Appl. Surf. Sci.* **2005**, *239*, 209.
(50) Headrick, J. E.; Armstrong, M.; Cratty, J.; Hammond, S.; Sheriff, B. A.; Berrie, C. L. *Langmuir* **2005**, *21*, 4117.
(51) Nuraje, N.; Banerjee, I. A.; MacCuspie, R. I.; Lingtao, Y.; Matsui, H. *J. Am. Chem. Soc.* **2004**, *126*, 8088.
(52) Liu, G. Y.; Xu, S.; Qian, Y. *Acc. Chem. Res.* **2000**, *33*, 457.
(53) Xu, S.; Miller, S.; Laibinis, P. E.; Liu. G. Y. *Langmuir* **1999**, *15*, 7244.
(54) Lutwyche, M. I.; Despont, M.; Dreschler, U.; Durig, U.; Haberle, W.; Rothuizen, H.; Stutz, R.; Widmer, R.; Binning, G. K.; Vettiger, P. *Appl. Phys. Lett.* **2000**, *77*, 3299.
(55) King, W. P.; Kenny, T. W.; Goodson, K. E.; Cross, G.; Despont, M.; Durig, U.; Rothuzien, H.; Binnig, G. K.; Vettifer, P. *Appl. Phys. Lett.* **2001**, *78*, 1300.
(56) Xiao, X.; Hu, J.; Charych, D. H.; Salmeron, M. *Langmuir* **1996**, *12*, 235.
(57) Mrksich, M.; Sigal, G. B.; Whitesides, G. M. *Langmuir* **1995**, *11*, 4383.
(58) Ostuni, E.; Chapman, R. G.; Holmlin, R. E.; Takayama, S.; Whitesides, G. M. *Langmuir* **2001**, *17*, 5605.
(59) Chapman, R. G.; Ostuni, E.; Yan, L.; Whitesides G. M. *Langmuir* **2000**, *16*, 6927.
(60) Gates, B. D.; Xu, Q.; Love, J.; Wolfe, D. B.; Whitesides, G. M. *Annu. Rev. Mater. Res.* **2004**, *34*, 339.
(61) Flynn, N. T.; Tran, T. N. T.; Cima, M. J.; Langer, R. *Langmuir* **2003**, *19*, 10909.
(62) Wanunu, M.; Vaskevich, A.; Cohen, R. S.; Hagai, C.; Arad-Yellin, R.; Shanzer, A.; Rubinstein I. *J. Am. Chem. Soc.* **2005**, *127*, 17877.
(63) Badyal, J. P. S. *Chem. Br.* **2001**, *37*, 45.
(64) Ryan, M. E.; Hynes, A. M.; Badyal J. P. S. *Chem. Mater.* **1996**, *8*, 37.
(65) Oye, G.; Roucoules, V.; Oates, L. J.; Cameron, A. M.; Cameron, N. R.; Steel, P. G.; Davis, B. G.; Coe, D. M.; Cox, R. A.; Badyal, J. P. S. *J. Phys. Chem. B* **2003**, *107*, 3496.
(66) Tarducci, C.; Kinmond, E.; Brewer, S.; Willis, C.; Badyal, J. P. S. *Chem. Mater.* **2000**, *12*, 1884.
(67) Hutton, S. J.; Crowther, J. M.; Badyal, J. P. S. *Chem. Mater.* **2000**, *12*, 2282.
(68) Tarducci, C.; Schofield, W. C. E.; Brewer, S.; Willis, C.; Badyal, J. P. S. *Chem. Mater.* **2001**, *13*, 1800.
(69) Teare, D. O. H.; Barwick, D. C.; Schofield, W. C. E.; Garrod, R. P.; Ward, L. J.; Badyal, J. P. S. *Langmuir* **2005**, *21*, 11425.
(70) Tarducci, C.; Schofield W. C. E.; Brewer, S. A.; Willis, C.; Badyal, J. P. S. *Chem. Mater.* **2002**, *14*, 2541.
(71) Tarducci, C.; Brewer, S. A.; Willis, C.; Badyal, J. P. S. *Chem. Commun.* **2005**, *3*, 406.

Table 1. Optimum Parameters for Pulsed Plasma Polymerization of Each Monomer

precursor	reactor temp (°C)	pulse duty cycle (μs)		deposition rate (nm min^{-1})
		time on	time off	
glycidyl methacrylate (+97%, Sigma-Aldrich)	22	20	20000	16
N-acryloylsarcosine methyl ester monomer (+97%, Lancaster)	22	20	5000	9
allyl mercaptan (+80%, Sigma-Aldrich)	40	100	4000	10

Table 2. Proteins and Their Associated Fluorophores Employed in This Study

protein	label	fluorophore
Protein G from streptococcus sp (Sigma-Aldrich)	Protein I	N/A
goat antimouse IgG (H + L) (Sigma-Aldrich)	Protein II	Alexa fluor 633
IgG from equine serum, salt-free (Molecular Probes)	Protein III	N/A
Protein A from staphylococcus aureus (Sigma-Aldrich)	Protein IV	FITC

Table 3. Contact Angle and XPS Elemental Composition of Pulsed Plasma Deposited Poly(*N*-acryloylsarcosine methyl ester), Poly(glycidyl methacrylate), and Poly(*N*-acryloylsarcosine methyl ester) Deposited on Top of Poly(glycidyl methacrylate)

pulsed plasma polymer(s)	contact angle (deg)	elemental composition		
		C %	N %	O %
N-acryloylsarcosine methyl ester	48 ± 3	63.1 ± 1.3	9.9 ± 0.4	26.9 ± 1.4
theoretical *N*-acryloylsarcosine methyl ester	N/A	64	9	27
glycidyl methacrylate	58 ± 1	68.9 ± 1.4		31.3 ± 1.3
theoretical glycidyl methacrylate	N/A	70	0	30
N-acryloylsarcosine methyl ester + glycidyl methacrylate	49 ± 4	63.1 ± 0.5	9.9 ± 0.3	26.9 ± 0.7

is achieved by switching monomers during pulsed plasma deposition. Subsequent removal of the outermost passivation layer by using a variety of micro- and nanoscale lithographic techniques leaves behind a patterned multifunctional surface, Scheme 1. An important attribute of this approach is that the decoupling of each pulsed plasma nanolayer deposition makes it remarkably cheap, quick, and efficient.

2. Experimental Section

2.1. Plasmachemical Nanolayering. Plasma polymerization was carried out in a cylindrical glass reactor (4.5 cm diameter, 460 cm^3 volume) located inside a Faraday cage and evacuated by a 30 L min^{-1} rotary pump via a liquid nitrogen cold trap (2×10^{-3} mbar base pressure and better than 1.2×10^{-9} mol s^{-1} leak rate). A copper coil (4 mm diameter, 10 turns, located 15 cm away from the precursor inlet) was connected to a 13.56 MHz radio frequency supply via an LC matching network. System pressure was monitored with a Pirani gauge. All fittings were grease free. During pulsed plasma deposition, the RF source was triggered by a signal generator, and the pulse shape monitored with an oscilloscope. Prior to each experiment, the apparatus was scrubbed with detergent, rinsed with propan-2-ol, and oven dried. Further cleaning entailed running a 40 W continuous wave air plasma at 0.2 mbar pressure for 20 min. At this stage, each monomer was loaded into a sealable glass tube and further purified using multiple freeze−pump−thaw cycles. The substrate of interest was then placed into the center of the reactor, and the system evacuated to base pressure. For each functional monomer, a continuous flow of vapor was introduced via a fine needle control valve at a pressure of 0.2 mbar and 1.5×10^{-7} mol s^{-1} flow rate for 5 min prior to electrical discharge ignition. Optimum pulsed plasma duty cycle parameters for each precursor are listed in Table 1. Upon completion of deposition, the RF power source was switched off and the monomer allowed to continue to purge though the system for a further 5 min prior to evacuation to base pressure and venting to atmosphere.

2.2. Protein Arrays. A bifunctional stack comprising pulsed plasma deposited protein-resistant poly(*N*-acryloylsarcosine methyl ester)[74] on top of protein-binding poly(glycidyl methylmethacrylate)[66] was employed for the preparation of protein arrays. Micrometer-scale protein patterns were fabricated using a computer-controlled robotic microarrayer (Genetix Inc.) equipped with micromachined pins delivering ~1 nL of protein solution onto the reactive pulsed plasma poly(glycidyl methacrylate) underlayer by puncturing the pulsed plasma poly(*N*-acryloylsarcosine methyl ester) protein-resistant top layer. Typical circular spots with diameters of 100−150 μm could be routinely prepared. Protein I and Protein III solutions were prepared by diluting in phosphate buffered saline (pH 7.0, Sigma-Aldrich) containing 40% v/v glycerol (+99%, Sigma Aldrich) to a final concentration of 20 μg mL^{-1}, Table 2. The spotted surfaces were incubated for 16 h at 22 °C in a humidified chamber (70% relative humidity). Protein immobilization occurred via reaction between the biomolecule amine groups and epoxide centers exposed during concurrent puncturing and liquid delivery.

Microarrays of Protein I and Protein III were subsequently exposed to solutions of fluorescently tagged complementary Protein II and Protein IV, respectively (20 μg mL^{-1} in phosphate buffered saline) for 60 min. This was followed by successive rinses in phosphate buffered saline, phosphate buffered saline diluted to 50% v/v with deionized water, and finally washed twice with deionized water.

Submicrometer scale protein immobilization entailed loading a molecular scratchcard onto an atomic force microscope stage (Digital Instruments Nanoscope III control module, extender electronics, and signal access module, Santa Barbara, CA). The protein-resistant pulsed plasma poly(*N*-acryloylsarcosine methyl ester) top layer was scratched away using a tapping mode tip (Nanoprobe, spring constant 42−83 Nm^{-1}) applied in contact mode. The movement of the tip in the *x*, *y*, and *z* plane was controlled by

(72) Coulson, S. R.; Woodward, I. S.; Brewer, S. A.; Willis, C.; Badyal, J. P. S. *Langmuir* **2000**, *16*, 6287.
(73) Schofield, W. C. E.; McGettrick, J.; Bradley, T. J.; Przyborski, S.; Badyal, J. P. S. *J. Am. Chem. Soc.* **2006**, *128*, 2280.
(74) Teare, D. O. H.; Schofield, W. C. E.; Garrod, R. P.; Badyal, J. P. S. *J. Phys. Chem. B* **2005**, *109*, 20923.

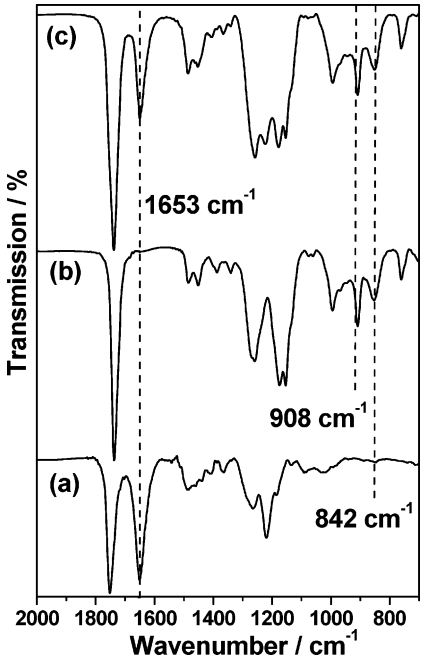

Figure 1. Infrared spectra of pulsed plasma deposited: (a) 20 nm poly(*N*-acryloylsarcosine methyl ester) protein-resistant layer; (b) 300 nm poly(glycidyl methacrylate) protein-binding layer; and (c) 20 nm poly(*N*-acryloylsarcosine methyl ester) on top of a 300 nm poly(glycidyl methacrylate) layer.

Veeco Nanolithography Software (version 5.30r1). The patterned molecular scratchcard was immersed in a solution of Protein I for 60 min at room temperature followed by successive rinses in phosphate-buffered saline, phosphate-buffered saline diluted to 50% v/v with deionized water, and twice with deionized water. The sample was then exposed to a complementary solution of Protein II (20 μg mL^{-1} in phosphate-buffered saline) for 60 min followed by successive rinses in phosphate-buffered saline, phosphate-buffered saline diluted to 50% v/v with deionized water, and finally washed twice with deionized water.

2.3. DNA Arrays. For the DNA arrays, poly(glycidyl methacrylate)[66] was employed as the passivation top layer, with poly(allyl mercaptan)[73] serving as the reactive underlayer. Scanning probe lithography was performed as described above. The patterned scratchcard was then immersed in a solution of thiol-terminated, Cy5-tagged, 15-base oligonucleotide (5′−AACGATGCACGAGCA−3′) diluted to a concentration of 400 nM in a 3 M sodium chloride (+99%, Sigma Aldrich)/0.5 M sodium citrate dihydrate (+99%, Sigma Aldrich) (SSC) buffer solution for 12 h at room temperature. This was followed by successive rinses in SSC, SSC diluted 50% v/v with deionized water, and twice in deionized water. Surface immobilization of the oligonucleotides occurred via disulfide bridge formation.[73]

2.4. Surface Characterization. X-ray photoelectron spectroscopy (XPS) was undertaken using an electron spectrometer (VG ESCALAB MK II) equipped with a non-monochromated Mg K$\alpha_{1,2}$ X-ray source (1253.6 eV) and a concentric hemispherical analyzer. Photoemitted electrons were collected at a takeoff angle of 30° from the substrate normal, with electron detection in the constant analyzer energy mode (CAE, pass energy = 20 eV). The XPS spectra were charge referenced to the C(1s) peak at 285.0 eV and fitted with a linear background and equal full-width-at-half-maximum (fwhm) Gaussian components[75] using Marquardt minimization computer software. Instrument sensitivity (multiplication) factors derived from

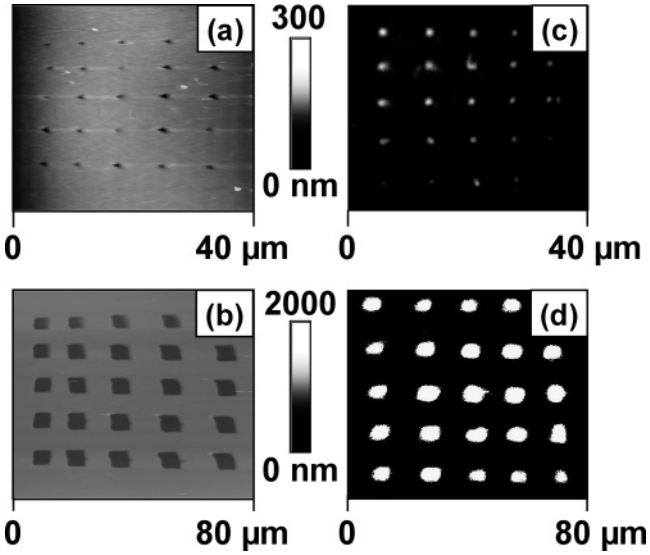

Figure 2. AFM micrographs of 5 × 5 arrays of exposed epoxide functionalities surrounded by a protein-resistant background: (a) 500 nm × 500 nm squares and (b) 5 μm × 5 μm squares. Corresponding fluorescence images following immersion of the functional array in Protein I, and then complementary fluorescent Protein II, are shown in (c) and (d), respectively.

chemical standards were taken as being 1.00:0.52:0.63:0.45 for C(1s):S(2p):O(1s):N(1s).

Fourier transform infrared (FTIR) analysis of the films was carried out using a Perkin-Elmer Spectrum One spectrometer equipped with a liquid-nitrogen-cooled MCT detector operating across the 700−4000 cm^{-1} range. Reflection−absorption (RAIRS) measurements were performed using a variable-angle accessory (Specac) set at 66° in conjunction with a KRS-5 polarizer fitted to remove the s-polarized component. All spectra were averaged over 516 scans at resolution of 1 cm^{-1}.

Contact angle analysis of the plasma-deposited films was carried out with a video capture system (ASE Products, model VCA2500XE) using 2.0 μL droplets of deionized water.

Film thickness measurements were carried out using an nkd-6000 spectrophotometer (Aquila Instruments Ltd). Transmittance−reflectance curves (over the 350−1000 nm wavelength range) were fitted to the Cauchy model for dielectric materials using a modified Levenburg−Marquardt method.[76]

AFM micrographs of each surface were acquired in the tapping mode[77] operating in air at room temperature (Digital Instruments Nanoscope III control module, extender electronics, and signal access module, Santa Barbara, CA).

Fluorescence microscopy was performed using an Olympus IX−70 system (DeltaVision RT, Applied Precision, WA). Image data was collected using excitation wavelengths at 525 and 633 nm corresponding to the absorption maxima of the dye molecules, FITC and Alexa Fluor 633, respectively.

3. Results

3.1. Protein Arrays. The XPS elemental stoichiometry of the pulsed plasma deposited poly(*N*-acryloylsarcosine methyl ester) protein-resistant film closely resembles the predicted theoretical composition calculated from the monomer structure, Table 3. Further confirmation of the high level of retained functionality was evident from the infrared

(75) Evans, J. F.; Gibson, J. H.; Moulder, J. F.; Hammond, J. S.; Goretzki, H. *Fresenius J. Anal. Chem.* **1984**, *319*, 841.
(76) Tabet, M. F.; McGahan, W. A. *Thin Solid Film* **2000**, *370*, 122.
(77) Zhong, Q.; Innis, D.; Kjollerm K.; Ellings, V. B. *Surf. Sci.* **1993**, *14*, 3045.

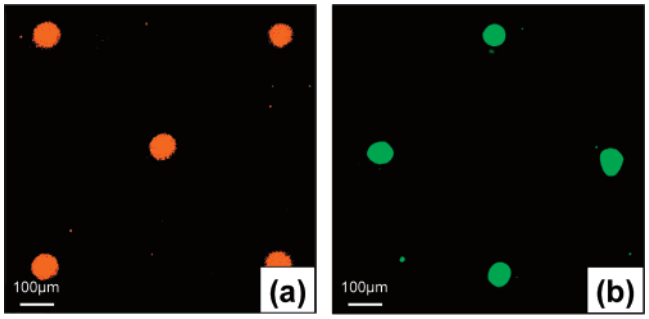

Figure 3. Fluorescence images of an alternating pattern of Protein I and Protein III after exposure to (a) Protein II and (b) Protein IV (scale bar is 100 μm).

spectrum, Figure 1a. Characteristic absorbances include 1749 cm^{-1} (ester carbonyl), 1653 cm^{-1} (amide), and 1212 cm^{-1} (ester C−O).[74]

A similar trend is observed for the pulsed plasma-deposited poly(glycidyl methacrylate) protein-binding layer, where XPS stoichiometry closely resembles the monomer composition, Table 3. Infrared spectroscopy indicates fingerprint absorption bands at 1728 cm^{-1} (ester carbonyl), 908 cm^{-1} (antisymmetric epoxide ring deformation), and 842 cm^{-1} (symmetric epoxide ring deformation), Figure 1b.[66]

Consecutive pulsed plasma deposition of a 300 nm thick poly(glycidyl methacrylate) layer followed by 20 nm of poly(*N*-acryloylsarcosine methyl ester) in the absence of cross-contamination was verified by infrared spectroscopy, Figure 1c. The antisymmetric epoxide ring deformation (908 cm^{-1}) and symmetric epoxide ring deformation (842 cm^{-1}) of poly(glycidyl methacrylate) are clearly visible, as well as the characteristic amide (1653 cm^{-1}) band of poly(*N*-acryloylsarcosine methyl ester). XPS composition and contact angle values of this bilayer stack were measured to be identical to those obtained for poly(*N*-acryloylsarcosine methyl ester), Table 3.

A regular 5 × 5 array of epoxide functionalities exposed through the protein-resistant layer was created by rastering an SPM tip across the bilayer surface to scratch either 500 nm × 500 nm squares or 5 μm × 5 μm squares, images a and b of Figure 2, respectively. Exposure of these functionally patterned surfaces to solutions containing Protein I and then complementary fluorescent Protein II verified that protein attachment to the exposed epoxide functionalities occurs in the correct configuration, Table 2 and images c and d of Figure 2.

Similarly, an alternating pattern of immobilized Protein I and Protein III, was prepared by concurrently puncturing the protein-resistant poly(*N*-acryloylsarcosine methyl ester) top layer and delivering the respective protein solution using a robotic microarrayer pin. Subsequent immersion in fluorescent Protein II solution displayed binding to Protein I only, Figure 3a, whereas exposure of the protein array to fluorescent Protein IV solution gave rise to exclusive binding to Protein III spots, Figure 3b.

3.2. DNA Arrays. XPS elemental analysis of pulsed plasma-deposited poly(allyl mercaptan) and poly(glycidyl methacrylate) films was found to be in good agreement with the theoretical precursor compositions, Table 4.[66,73]

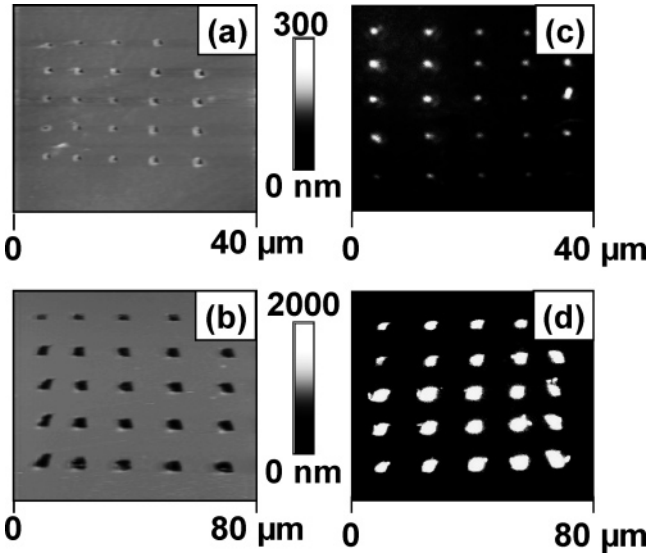

Figure 4. AFM micrographs showing a 5 × 5 array of exposed thiol functionalities surrounded by epoxide background: (a) 500 nm × 500 nm squares and (b) 5 μm × 5 μm squares. Corresponding fluorescence images following immersion in Cy5-tagged, thiol-terminated DNA are shown in (c) and (d), respectively.

Pulsed plasma deposition of a 300 nm thick poly(allyl mercaptan) DNA binding layer followed by a 20 nm thick poly(glycidyl methacrylate) nonbinding film was verified by XPS elemental composition and contact angle values of the bilayer stack matching poly(glycidyl methacrylate).

A regular 5 × 5 array of exposed thiol functionalities was created by rastering an SPM tip to scratch either 5 μm × 5 μm or 500 nm × 500 nm squares, images a and b of Figure 4, respectively. Exposure of these patterned surfaces to thiol-terminated, Cy5-tagged oligonucleotide demonstrated the reactivity of the exposed poly(allyl mercaptan) pixels, images c and d of Figure 4, respectively. Clearly, such arrays can be utilized for DNA hybridization and rewriting applications by using previously reported protocols.[73]

4. Discussion

A functional protein array typically comprises a series of protein spots immobilized onto a solid surface while retaining biological functionality.[6−8] Numerous approaches have been devised to facilitate this,[78] including covalent attachment to activated surfaces through reactive linker groups,[79,80] gel-coated slides,[81] and affinity capture of proteins via biomolecular interactions.[82] However, all of these methods suffer from either restriction to the utilization of only one protein[83] or the limitation of nonspecific protein adsorption onto the

(78) Heng, Z.; Snyder, M. *Curr. Opin. Chem. Biol.* **2003**, *7*, 55.
(79) Zhu, H.; Klemic, J. F.; Chang, S.; Bertone, P.; Casamayor, A.; Klemic, K. G.; Smith, D.; Gerstein, M.; Reed, M. A.; Snyder, M. *Nat. Genet.* **2000**, *26*, 283.
(80) Wilson, D. S.; Nock, S. *Curr. Opin. Chem. Biol.* **2001**, *6*, 81.
(81) Arenkhov, P.; Kukhtin, A.; Gemmell, A.; Voloschuck, S.; Chupeeva, V.; Mirzabekov, A. *Anal. Biochem.* **2000**, *278*, 123.
(82) Zhu, H.; Bilgin, M.; Bangham, R.; Hall, D.; Casamayor, A.; Bertone, P.; Lan, N.; Jansen, R.; Bidlingmaier, S.; Houfek, T.; Mitchell, T.; Miller, P.; Dean, R. A.; Gerstein, M.; Snyder, M. *Science* **2001**, *293*, 2101.
(83) Lee, S. W.; Oh, B. K.; Sanedrin, R. G.; Salaita, K.; Fujigaya, T.; Mirkin, C. A. *Adv. Mater.* **2006**, *18*, 1133.

Table 4. Experimental Contact Angle and Composition of Pulsed Plasma Deposited Poly(allyl mercaptan), Poly(glycidyl methacrylate), and Poly(glycidyl methacrylate) Pulsed Plasma Deposited onto Poly(allyl mercaptan)

		elemental composition		
pulsed plasma polymer(s)	contact angle (deg)	C %	S %	O %
allyl mercaptan	83 ± 4	72.4 ± 2.2	27.6 ± 2.2	0
theoretical allyl mercaptan	N/A	75	25	0
glycidyl methacrylate	59 ± 2	66.9 ± 1.1	0	33.1 ± 1.1
theoretical glycidyl methacrylate	N/A	70	9	30
glycidyl methacrylate + allyl mercaptan	61 ± 2	66.6 ± 0.3	0	33.3 ± 0.6

surrounding background,[84,85] leading to a reduction in background fluorescence (rather than complete elimination of nonspecific protein binding). The molecular scratchcard protein arrays described in this article utilize a bifunctional pulsed plasma nanolayer stack comprising a 20 nm pulsed plasma-deposited poly(*N*-acryloylsarcosine methyl ester) protein-resistant top coating[74] and a 300 nm pulsed plasma deposited poly(glycidyl methacrylate) underlayer containing reactive epoxide groups amenable to binding primary amine groups belonging to the protein[86,87] via nucleophilic attack. It has been shown that the top layer can be pierced using a robotic microarrayer pin to concurrently deliver approximately 1 nl droplets of protein solution direct to the underlying reactive epoxide surface. Retention of protein functionality has been demonstrated by generating an alternating array of Protein I and Protein III, which bind selectively to fluorescently labeled Protein II[88] and Protein IV,[89] respectively, Figure 3. An important attribute of this nanolayered functional stack is that it benefits from low background fluorescence due to the elimination of nonspecific protein adsorption as a consequence of the protein-resistant top layer. In a similar fashion, the utilization of an SPM probe tip can provide much smaller (higher density) arrays. Further variants could include the marrying of this molecular scratchcard concept with dip pen nanolithography. Also, smaller scale features are feasible by utilizing sharper SPM tips (e.g., carbon nanotubes).

To demonstrate the versatility of molecular scratchcards, we also performed the immobilization of deoxyribonucleic acid (DNA). The fabricated molecular scratchcard DNA array utilizes a dual pulsed plasma nanolayer stack comprising a 300 nm pulsed plasma poly(allyl mercaptan) underlayer possessing reactive thiol groups amenable to binding to thiol-terminated DNA strands and a 20 nm pulsed plasma top-coating of poly(glycidyl methacrylate), which does not bind to thiol-terminated DNA (thus acting as a passivation layer). Selective removal of the poly(glycidyl methacrylate) outer layer exposes the underlying thiol linker groups. Fluorescently tagged thiol-terminated DNA strands have been shown to readily react with these sites via disulfide bridge formation. Such immobilized DNA strands can then undergo hybridization with their complementary strands.[73]

5. Conclusions

Pulsed plasmachemical nanolayering is a relatively straightforward method for the fabrication of multilayer functional stacks. Sequential deposition of a reactive layer and then a passivation layer, followed by selective localized unveiling of the underlying reactive groups by piercing the passive top layer, has been shown to be an effective way of preparing protein and oligonucleotide arrays.

CM0624670

(84) Vroman, L.; Adams, A. L.; Fischer, G. C.; Munoz, P. C. *Blood* **1980**, *55*, 156.
(85) Wang, M. S.; Palmer, L. B.; Schwarts, J. D.; Razatos, A. *Langmuir* **2004**, *20*, 7753.
(86) Deng, Y.; Zhu, W. Y.; Kienlen, T.; Guo, Q. *J. Am. Chem. Soc.* **2006**, *128*, 2768.
(87) Mateo, C.; Torres, R.; Fernandez-Lorente, G.; Ortiz, C.; Fuentes, M.; Hidalgo, A.; Lopez-Gallego, F.; Abian, O.; Palomo, J. M.; Guisan, J. M.; Betancor, L.; Pessela, B. C. C.; Fernandez-Lafuente, R. *Biomacromolecules* **2003**, *4*, 772.
(88) Lindmark, R.; Thoren-Tolling, K.; Sjoquist, J. *J. Immunol. Methods* **1983**, *62*, 1.
(89) Bjorck, L.; Kronvall, G. *J. Immunol.* **1984**, *133*, 969.